

Practical guidelines for choosing GLCM textures to use in landscape classification tasks over a range of moderate spatial scales

Mryka Hall-Beyer

To cite this article: Mryka Hall-Beyer (2017) Practical guidelines for choosing GLCM textures to use in landscape classification tasks over a range of moderate spatial scales, International Journal of Remote Sensing, 38:5, 1312-1338, DOI: [10.1080/01431161.2016.1278314](https://doi.org/10.1080/01431161.2016.1278314)

To link to this article: <https://doi.org/10.1080/01431161.2016.1278314>



Published online: 31 Jan 2017.



Submit your article to this journal 



Article views: 2649



View related articles 



View Crossmark data 



Citing articles: 86 View citing articles 



TECHNICAL NOTE

Practical guidelines for choosing GLCM textures to use in landscape classification tasks over a range of moderate spatial scales

Mryka Hall-Beyer

Department of Geography, University of Calgary, Calgary, Canada

ABSTRACT

Texture measurements quantitatively describe relationships of DN values of neighbouring pixels. The output is a continuous measure of spatial information that may be used for further processing. Spatial relationships are not necessarily correlated with spectral data for a given class, and including a measure of them improves classification accuracy. This research develops a guideline for choosing among the Haralick (Grey Level Co-occurrence Matrix [GLCM]) set of texture measures. These guidelines are derived using a variety of land covers and spatial scales (window sizes).

Principal component analysis (PCA) of eight GLCM measures was performed for three Landsat TM and ETM+ images: a mid-latitude agricultural and natural vegetation scene, a glacier–rock–sea ice scene, and a desert scene with dunes and structurally complex rocks. PCA was performed separately for neighbourhoods consisting of squares with 25, 13, and 5 pixels on a side to demonstrate robustness to different spatial scales. PCA loadings show that contrast (Con), dissimilarity, entropy (Ent), and GLCM variance are most commonly associated with visual edges of land-cover patches; homogeneity, GLCM mean, GLCM correlation (GLCM Cor), and angular second moment are associated with patch interiors. Edge-highlighting textures account for most dataset variance but fail to differentiate among classes. Eigenchannels highlighting patch interior characteristics rely on GLCM mean and to some extent GLCM Cor. These two textures do contribute to distinguishing individual class signatures for classification purposes. Ent does not appear consistently in edge or interior groupings. Ent is interpreted as important to the textures of particular classes, but which classes is not generalized from one scene to another. Con is effective for outlining patch edges and may serve for object formation in geographic object-based image analysis (GEOBIA).

For classification purposes, the proposed guideline is a choose Mean and, where a class patch is likely to contain edge-like features within it, Con. Cor is an alternative for Mean in these situations, Dis may similarly be used in place of Con. For more detailed texture study, add Ent. This guideline does not constitute a complete texture analysis but may allow confident use of GLCM texture to enhance the efficiency of Landsat-based classification.

ARTICLE HISTORY

Received 15 July 2016
Accepted 23 December 2016



1. Introduction

'Texture' is quantified by a set of continuous variables, which describes the local spatial arrangement of reflectance values. The output is a single raster layer that contains these measurements for all pixels and may be input into further analysis. Texture layer(s) add quantitative spatial information to per-pixel classifications. Since some texture measures brighten pixels located at the boundary of patches of single ground cover classes, texture has the potential to be an important data input to create multi-pixel objects in object-based analysis. Texture as defined visually has long been an important element in visual image interpretation, allowing operators to separate spectrally similar image regions. In visible and infrared-wavelength remotely sensed images, texture provides information that is independent of spectral reflectance values. Therefore, inclusion of a texture band often improves classification accuracy, no matter what approach or decision rule is used (Marceau et al. 1990; Ferro and Warner 2002; Colombo et al. 2003; Myint, Lam, and Tyler 2004).

Until the advent of automated image processing systems, 'texture' was ill defined and left to the individual interpreter. It was characterized by terms such as 'mottled' or 'rough' (Lillesand, Kiefer, and Chapman 2007; Jensen 2007). For computer-based classification, a numeric representation of texture is required. The seminal work in numerical texture for image interpretation was provided by Haralick in the 1970s (Haralick, Shanmugam, and Dinstein 1973; Haralick 1979). Particularly in the period 2000–2010, many different texture approaches were pioneered; Table 1 provides a representative sample. None of these has replaced Grey Level Co-occurrence Matrix [GLCM] on a widespread basis. Haralick's texture measures remain widely implemented in software and are able to incorporate multiple elements of texture. As noted by Wang et al. (2016), the primary improvements in GLCM since the 1970s have resided in faster calculation algorithms, rather than changes in the statistics themselves.

GLCM texture has been proved to be successful in many classification activities, increasing classification accuracies. It has been used extensively in forestry, where shadow patterns caused by different tree structure give rise to distinctive textures (Franklin et al. 2000). Its utility has been corroborated for high spatial resolution as well as moderate resolution images (Ozdemir and Karnieli 2011; Murray, Lucieer, and Williams 2010; Ozdemir and Donaghue 2013; Rabia and Terribile 2013). In other land covers, GLCM texture has recently been used to interpret landscape metrics (Ozdemir, Mert, and Senturk 2012) and geomorphological patterns (Okubo et al. 2010). GLCM texture has been incorporated into object classification in GEOBIA applications (Kim,

Table 1. Various texture approaches.

Authors	Year	Approach
Chen and Gong	2004	Variogram parameters
Dong	2000	Lacunarity estimation
Emerson, Lam, and Quattrochi	2005	Variance, Fractals, and Moran's I
Myint	2003	Fractals, autocorrelation, descriptive statistics
Myint et al.	2004	Wavelets compared to fractal, autocorrelation, GLCM
Pearlstine, Portier, and Smith	2005	First and second-order (GLCM) statistics, edge density
Rushing et al.	2001	Association rules
Srinivasan and Shobha	2008	Various non-GLCM statistics

Madden, and Warner 2009; Rabia and Terribile 2013); however, texture may also help define edges when forming geographical objects (Okubo et al. 2010). The idea is that particular texture measures produce contrasting (bright or dark) pixels where textures change, in other words on natural patch (object) edges. When the object-creating algorithm encounters such prominent pixels in the texture layer, adding these pixels to existing objects would cause a large increase in within-object variance, thus stopping object enlargement at an appropriate place.

1.1. Definitions of texture

Because it characterizes pixel DN value variation over space, texture must be calculated in a neighbourhood consisting of multiple pixels. Within this neighbourhood, texture has three elements: tonal (DN) difference between pixels, the distance over which this difference is measured, and directionality. These are also conceptualized as smoothness, coarseness, and regularity (Gonzalez and Woods 1992). The number of pixels included in a neighbourhood can be varied. This affects the resulting measure because a single calculation neighbourhood may include edges or patches with different textures, especially for larger neighbourhoods. Most implementations allow the user to define the neighbourhood, which for practical reasons is usually a square area called a window or kernel. The window has an odd number of pixels on a side. Occurrence or first-order texture measures, such as variance, consider all the pixel values within the neighbourhood but do not account for their spatial relationships to one another (Haralick, Shanmugam, and Dinstein 1973) First-order measures, particularly within-window variance, can successfully distinguish textures which characterize some land covers. They have the advantage of simplicity of concept and calculation (Ferro and Warner 2002). Several window sizes may be included for detailed textural analysis where this is desirable (Coburn and Roberts 2004).

Haralick's GLCM textures are co-occurrence or second order. They are based on tonal (DN) differences between pairs of pixels in a spatially defined relationship and consider all pixel pairs within the neighbourhood. A simple example is that second-order measures can distinguish vertical stripes two pixels wide from stripes one pixel wide, given uniform DN values in each stripe; first-order textures could not do this. The GLCM has the advantage of being able to account for all three texture elements; although in practise, distance is usually defaulted to the image's spatial resolution (1 pixel) and directionality is usually defaulted to omnidirectional unless directionality is the subject of the investigation. The research reported here accepts these most common defaults as suitable for its purpose of illuminating texture measure selection for classifying a wide variety of images.

Each texture measure is calculated using one input layer, chosen by the user, and yields one output layer. If multiple inputs and many measures are desired, many new bands are produced. While having many bands provides flexibility, engaging in a systematic selection is an entire project in itself (Murray, Lucieer, and Williams 2010; Laurin et al. 2013). Being faced with so many choices may deter the user who wishes to gain the advantage of independent spatial data, without engaging in texture research. By default, a single band which contains most contrast for a given image is often chosen as the substrate for texture calculation. An alternative is to calculate texture starting

from an index such as NDVI or a first principal component containing a large percentage of total variance across all bands. There are quantitative helps to choosing neighbourhood size, for example using semivariogram range to determine dominant patch and hence window size(s). In some places, local geographical knowledge may suggest appropriate sizes, for example common field sizes in agricultural areas (Okubo et al. 2010). Since many images contain several patch sizes, more than one window size may be considered. Choice of window size is extensively discussed in Dorigo et al. (2012) and Franklin et al. (2000).

Once input band and window size are chosen, the measure(s) to use must be chosen. GLCM textures can tackle all dimensions of texture simultaneously. This article reports the results of a systematic empirical investigation of the relation among the most commonly implemented GLCM measures for three very different landscapes using Landsat images. It does not claim to solve all questions. It advances theoretical knowledge of the Haralick or other textures only to the extent that it shows the rules of thumb are logically consistent with the calculations defining the GLCM. It intends to recommend the best choice of texture for those wishing to add independent information about spatial relationships to a classification, without engaging in an in-depth analysis of texture itself.

1.2. Haralick textures

The GLCM is a matrix which tallies frequencies of associations of values for pairs of pixels within a neighbourhood, normalized to probabilities. It is thus entirely data dependent and should be thought of as a descriptive statistic. Numerical values cannot be compared across images. Many statistical texture measures can be calculated from the GLCM. Haralick (1979) suggested 14, but not all are implemented in common software: PCI Geomatica uses nine, plus minor variations on four of these (PCI 2013); ENVI uses eight (RSI 2004) and MATLAB has built-in code for four (MathWorks graycoprops 2012). Eight are considered in this article, listed in Table 2.

1.2.1. Correlation among measures due to definitions

Because of the calculation method, many of these measures are highly correlated with one another. For example, the only difference between Con and Dis is the rate of decay of the weight given to GLCM entries as they become farther away from the matrix diagonal (the (i and j) value in Table 2 equations). The weight is the square of the distance in Con and the absolute value of the distance in Dis. The equations themselves indicate that the two should be non-linearly correlated. In practise, most image texture values do not fall at the extremes, and a typical empirical linear correlation coefficient between these two measures is >0.9. The actual value differs from image to image, depending on the landscape and neighbourhood size, but is rarely much lower.

Because of the similarity of calculation, correlation is also expected to be high between

- Entropy (Ent) and angular second moment (ASM) (negative correlation expected),
- Dis and Con (positive),
- Homogeneity (Hom) and Dis, also Hom and Con (negative).

Table 2. Texture measures used in this article, their abbreviations and equations, after PCI (2013).

Referred to as	Texture measure name	Calculation formula
Hom	Homogeneity	$\sum_{i,j=0}^{N-1} (P_{i,j}/1 + (i-j)^2)$
Con	Contrast	$\sum_{i,j=0}^{N-1} P_{i,j}(i-j)^2$
Dis	Dissimilarity	$\sum_{i,j=0}^{N-1} P_{i,j} i - j $
Mean	GLCM Mean	$\mu_i = \sum_{i,j=0}^{N-1} i(P_{i,j}) \mu_j = \sum_{i,j=0}^{N-1} j(P_{i,j})$
Var	GLCM variance (calculated as standard deviation in some software)	$\sigma_i^2 = \sum_{i,j=0}^{N-1} P_{i,j}(i - \mu_i)^2; \sigma_j^2 = \sum_{i,j=0}^{N-1} P_{i,j}(j - \mu_j)^2 \sigma_i = \sqrt{\sigma_i^2}; \sigma_j = \sqrt{\sigma_j^2}$
Ent	Entropy	$\sum_{i,j=0}^{N-1} P_{i,j}(-\ln P_{i,j})$
ASM	Angular second moment	$\sum_{i,j=0}^{N-1} P_{i,j}^2$
Cor	GLCM correlation	$\sum_{i,j=0}^{N-1} P_{i,j} \left[(i - \mu_i)(j - \mu_j) / \sqrt{(\sigma_i^2)(\sigma_j^2)} \right]$

For detailed explanations of calculations, see Hall-Beyer (2007) and Gonzalez and Woods (1992).

$P_{i,j}$ is the probability of values i and j occurring in adjacent pixels in the original image within the window defining the neighbourhood. i and j are the labels of the columns and rows (respectively) of the GLCM. Because of the construction of the GLCM, i refers to the DN value of a target pixel, and j is the DN value of its immediate neighbour (rook's case). In the GLCM Cor equation, μ is the mean and σ the standard deviation, both as defined by the equations for GLCM Mean and GLCM Var in the table.

Also because of the calculation method, some of the Haralick textures, particularly GLCM correlation (Cor) and GLCM mean (Mean), are expected not to be highly correlated with any others. Finally, one would expect that Ent (conceptualized as unpredictability or irregularity) and Hom (uniformity) would be negatively correlated, although this is not immediately apparent from the equations alone. One common guideline for choosing which measure to use is to choose one measure from each of the uncorrelated groups (Hall-Beyer 2007; Murray, Lucieer, and Williams 2010; Ozdemir and Donaghue 2013). Another guideline might be to eliminate any measure that is highly correlated with any other measure. These guidelines do not help with choosing within a group. The principal component analysis (PCA) conducted below is designed to find out which measures are most commonly associated over different landscapes, to test and improve upon these guidelines.

1.3. Edge and interior textures

The equations in Table 2 predict several things. The group of Dis, Con, Ent, and Var can be referred to as *edge textures*. These yield high values when the neighbourhood contains visual edges, i.e. abrupt changes in DN values between neighbouring pixels. A true edge in the landscape would have some spatial coherence to contrasting pixel pairs. Such a continuous edge would mean that many pixel pairs within the neighbourhood have large differences, and these texture measures will record a high value for the neighbourhood. From their names, it is evident that Con and Dis fall into this category. GLCM variance (Var) should take on higher values for neighbourhoods containing visual edges but may also have high values in areas of incoherent (non-edge) high variability.

Higher Ent values would be recorded for neighbourhoods containing very irregular edges or incoherent contrast, whereas straight-line edges would lower Ent values for the neighbourhood. Few continuous straight edges which occur in natural environments, they are more common in human-dominated landscapes. Therefore, Con and Dis may have interesting relationships with Ent or Var.

Other texture measures yield high values for a neighbourhood which contains few coherent edges but has many subtle and irregular variations. These textures would be Hom, ASM, Cor, and Mean plus possibly Var as explained above. These can be termed *interior* textures, being able to take on values characterizing area away from coherent edges. Examples of classes probably best characterized by interior textures would be forest, undeformed rock, agricultural fields, or water. Each would have a unique range of texture values that could be used to identify it.

Despite the convenience of calling textures either 'edge' or 'interior,' some areas that users would be likely to define as a single ground cover patch are full of visual edges, even in their 'interiors.' Examples would be the sand dunes in the LB image and the iceberg-laden waters of the GR image described below plus perhaps the dendritically drained grasslands on the AB image. What is edge and what is interior depends on the image's spatial resolution relative to the way the ground class is conceptualized. For example, individual trees would be internal variability to a 'forest' class on a medium-resolution image but edges on a high-resolution image for the class 'oak tree.'

1.4. Principal components

One approach to using texture in image classification is to produce a suite of texture images at various neighbourhood sizes and measures and then calculate the principal components of the output channels. There are two problems with this approach. First, the operator must still make subjective choices about which measures and how many window sizes; reasonable limitations would still include hundreds of possibilities. Second, PCA is data dependent and isolates variation types in individual components. The user must still interpret the PCA output to decide which component to include in classification. Using multiple-texture input to PCA works well when texture is a major object of the research. When texture is desired simply to improve classification, using PCA is inefficient and daunting, as well, it still requires many choices which cannot be proven optimal. As a result, classifications may fail to include texture from simple user frustration.

In this article, PCA is used for a different purpose: to derive guidelines which allow texture to be more efficiently included in this type of problem. The reasoning is as follows

- (1) PCA is data dependent. Let us then produce a large variety of textures and use several different window sizes on several images with very different ground covers. PCA is used to extract common patterns among all the trials.
- (2) If PCA shows that commonalities occur in many or all of these trials, then we may propose practical guidelines for selection of a small number of textures.
- (3) Since we are in the realm of descriptive statistics, validation occurs by showing logical consistency between the texture measure calculation methods and the

rules. Further validation can occur by noting success in improving classification using the selected texture measures in previously published research, and going forward by those classifications that succeed when using the rules derived. Absolute optimality of these choices in all circumstances cannot be demonstrated, just as absolute optimality of choice of a classification decision rule for a given situation cannot be demonstrated.

This procedure follows from the commonalities which are observed among different images when PCA is performed using spectral data. For example, in spectral PCA, the first eigenchannel, PC1, usually indicates the multiband albedo common to all ground classes or brightness. For most spectral PCA, one or more of the subsequent eigenchannels usually represents vegetation, providing that some exists on the image. Temporal PCA also yields commonalities over different image-set inputs. PCA of temporal images using multi-date NDVI usually results in PC1 representing overall vegetation density (greenness) and PC2 representing the degree of seasonality (Eastman and Fulk 1993; Hall-Beyer 2003). With these findings, PCA using texture inputs is anticipated to yield commonalities across images and scales.

1.5. Interpreting PCA loadings

The key to identifying commonalities among PCA results is interpreting loadings (also known as factor scores or factor loadings) and eigenvalues output by PCA (Jolliffe 2002). Loadings record the correlation between individual input bands (texture measures) and the individual eigenchannel (component channel). Since loading interpretation forms the basis of generalizations and guideline formation below, this section presents a brief outline of its principles.

- A group of input bands may all have high positive correlation with a particular eigenchannel. This means that the eigenchannel has a high output pixel DN value (appear bright) for pixels where *all* of these highly loaded bands have high values for that pixel (and *vice versa*: low pixel values where all highly loaded inputs are low). Highly negatively loaded eigenchannels show low values (appear dark) where all the highly negatively loaded bands have high values (appear bright) and *vice versa*.
- An eigenchannel may show high loadings of opposite sign for different inputs. A bright pixel in such an eigenchannel is simultaneously bright in a positively loaded input and dark in a negatively loaded input. A well-known spectral example is a ‘vegetation’ eigenchannel with high positive loadings for a near-infrared band and high negative loadings for visible bands. Put another way, an eigenchannel with high positive and negative loadings to different inputs represents a ground feature showing contrast between these inputs in the original data. Eigenchannels with this loadings pattern are analogous to ratio spectral indices.
- A loading near 0, whether positive or negative, indicates no relevance of that input for the eigenchannel. However, the definition of ‘near 0’ must be in relation to the other loadings for a particular eigenchannel. This is because successive eigenchannels record successively lower portions of the total dataset variance (eigenvalues); hence, maximum loadings for any input will decrease in later eigenchannels. The last few

eigenchannels, with very low eigenvalues and very low maximum loadings, usually represent noise, i.e. variability uncorrelated with anything meaningful in the image.

1.6. Objective

The objective of this study is to develop a practical rule for choosing among available GLCM texture measures for incorporation into classification routines. The rule is developed using PCA to explore commonalities of textural PCA using eight GLCM texture measures and three different neighbourhood sizes. It uses PCA's data dependency to draw widely applicable generalizations by using images containing extremely different ground covers. If all three images, and all three neighbourhood sizes, allow the same generalizations, it is hypothesized that they derive from the nature of the various texture measures themselves and can be applied to any scene. It is expected that texture measures with equation-induced correlations as described above in [Section 1.2.1](#) will be consolidated into the first few eigenchannels, but other predictions cannot be made at the outset.

1.6.1. Limitations

This is an empirical study because texture selection for ordinary classification in practise is a matter of informed guessing. Individual application areas have suggested textures for particular studies, but there is no systematic universal relation between a given ground cover and a given texture. This study seeks commonalities among many ground covers in order to better guide these selections. It does not seek to demonstrate universality of its finding to all images and all ground covers. Specifically, the study examines Landsat data and so does not consider the effect of different spatial scales, beyond the selection of window sizes. Neither does it consider land covers not definable using Landsat spatial and spectral characteristics. It does not derive any relationship between particular ground covers and textures, only examines the function of the texture measures relative to one another. It also does not examine the effects of different pixel-pair spacing or directionality in the GLCM construction. The results are intended to serve as broad guidelines for texture measure selection in classification exercises. In cases where texture itself is the object of the research, or where very subtle textural differences are important, a closer analysis of the individual image considering many textures will need to be undertaken. Finally, this study does not relate texture measure selection to radar speckle, which has causes unrelated to ground cover and so needs to be investigated separately.

1.7. Methods

1.7.1. Data

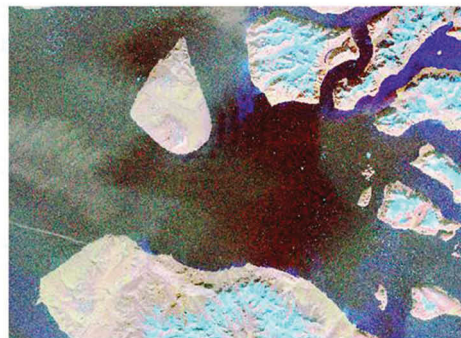
Generalizations were developed and stated as hypotheses using a mid-latitude scene with typically varied land covers: forest, irrigated and non-irrigated cropland, pasture, small urban areas, and native grasslands with well-developed dendritic drainage. The hypotheses were then tested on two scenes of very different landscape composition and location, described below. Texture was performed on one band only in each

image. The band was chosen to show high contrast for most of the ground covers, chosen visually. A systematic way of choosing appropriate bands for spatial analysis has been explored in Xianghai Cao et al. (2016). The development image is Landsat 7 ETM+ path 40/row 25, acquired on 27 July 1999 in a grassland and agricultural region near Medicine Hat, Alberta, Canada. This is referred to below as the AB (Alberta) image. Analysis was performed on ETM+ band 4 (near infrared). One test image is Landsat 7 ETM+ path 13/row 10 acquired on 4 August 2001, referred to below as GR (Greenland). ETM+ band 3 is used. GR contains sea ice, land-fast glaciers, and bare rock without coherent deformation patterns. The second test image is Landsat 5 TM path 190/row 41 acquired on 2 January 1987 (TM band 4 used), referred to below as LB (Libya). LB contains non-vegetated desert including sand dunes and bare deformed bedrock. All images were subset to 4000×3000 pixels, to remove background pixels. All images were downloaded from the Global Land Cover Facility at the University of Maryland (<http://glcf.umiacs.umd.edu/data/>) and not subjected to further processing. Figure 1 shows each image in a visually informative false-colour

(a) AB Image: centre $50^{\circ}07'20''$ N,
 $111^{\circ}30'18''$ W



(b) GR Image: centre $70^{\circ}59'36''$ N,
 $53^{\circ}12'56''$ W



(c) LB Image: centre $27^{\circ}14'56''$ N,
 $9^{\circ}41'56''$ E



30 km



Figure 1. (a) AB false-colour image, with TM bands 3, 2, and 1 as red, green, and blue (RGB). The darker square feature in NE corner occurs on the landscape and is not an image artefact. (b) GR image, RGB = TM bands 7, 4, 3 (cyan speckles are icebergs; line at lower left is a contrail). (c) LB image, RGB = TM bands 7, 4, 2. North and scale bar apply to all images.

composite. None has visible atmospheric interference in the bands chosen, with the exception of a contrail crossing the GR image.

1.7.2. Software and calculations

Texture calculations were carried out using PCI Geomatica v. 10.3 using 4-bit quantization and an isotropic directional relationship. PCA was performed using ENVI v. 4.8. Eigenvectors that were calculated using the correlation rather than the covariance matrix (standardized PCA). This eliminates any potential bias arising from different dynamic ranges of different input band values (Eklundh and Singh 1993; Ricotta and Avena 2000). Loadings are read directly from the eigenvectors when conducting standardized PCA. The quantization level was chosen as the one most commonly used in commercially available software at the time of the experiment. Some software does permit 5-bit quantization, but as this is not readily available, nor has it been conclusively demonstrated to be superior to 4-bit, 4-bit was used here.

The final possible choice when calculating GLCM texture is the pixel spacing. For this article, the default value of adjoining pixel pairs in any direction was used. There is no indication in the literature that varying pixel spacing (e.g. comparing a pixel's DN with that of pixels two or three pixel distance, rather than adjoining) accomplishes anything in images of natural scenes. The effect might be supposed to be a form of degrading the spatial resolution, which would serve no logical purpose in an experiment of this kind.

The eight textures calculated for the AB image and input into the PCA are shown in **Table 2**. Calculations were performed on all images using a 25×25 (56 ha) pixel window. This window size calculates the GLCM considering 312 pairs of pixels. Calculations were repeated using 5×5 (2.25 ha) and 13×13 (15.21 ha) window sizes. These sizes were chosen to bracket likely ground cover patch sizes on Landsat images so that each size should have some windows entirely within a patch. Images are referred to below using their location abbreviation (AB, GR, or LB) and the size of the neighbourhood in use (25, 13, or 5). Thus, 'AB25' for example refers to the texture images calculated using the AB image as input and a 25×25 pixel window size.

Eigenchannels (referred to below as components) were visually categorized as either emphasizing edges ('edge components') or not ('interior components') on the output image as a whole. This terminology should be distinguished from the groupings of 'edge' and 'interior' texture measures predicted above from the texture equations. The two are expected to be related (i.e. edge components will be heavily loaded with edge textures and interior components with interior textures), but this is an item to be tested, not an assumption. Loadings were examined to look for input textures which appear most commonly on each component type. Hypotheses were generated based on patterns in the development (AB) image and tested by determining their applicability to the two test images at the 25 pixel neighbourhood. The hypotheses were then tested against the 13 and 5 pixel neighbourhood sizes for all three images. From these analyses, generalizations were made to arrive at a unified guideline for choosing which texture measures to include in a wide range of ordinary classification procedures.

2. Results and discussion

This section presents the data used to form and test the generalizations. For each image and each window size, the following information is provided to support the arguments

- Table of eigenvalues for the components. The purpose is to identify which components contain a sufficient portion of the input variance to be considered for further analysis. Edge and interior assignment by visual observation, as illustrated by the image figures, is included in these tables for convenience.
- Graphical presentation of loadings values for each input texture for the components considered. [Section 1.4](#) briefly explains how loadings are used to identify the information content of each component. These are the primary interpretive tools to form and test the hypotheses.
- Table of correlations among original input texture bands. The purpose is to demonstrate the degree to which the correlations anticipated from texture equations actually occur in the image in question, as introduced in [Section 1.2.1](#). This further illuminates the loadings.
- Figures showing the output components to illustrate their assignment as edge or interior components.

2.1. Hypothesis development: Alberta image 25 × 25 window size (AB25)

Distribution of dataset variance is found in [Table 3](#). [Figure 2](#) illustrates that PC1 and PC3 emphasize edges and PC2 and PC4 interiors, as defined above.

For this image, 'edge' components account for a much larger portion of total texture variability 68.03% than do 'interior' components (29.14%) ([Table 3](#)). This leads to the first hypothesis

Hypothesis 1: Edge components account for a much larger percentage of total dataset variance than interior components.

This implies that PC1, with the largest portion of dataset variance, will be an edge component.

[Figure 3](#) shows loadings for each of the first four PCs. The loadings for PC1 for this image are predictable from the overall correlation matrix of the eight input textures, shown in [Table 4](#).

All of the edge textures are negatively correlated with interior textures but positively correlated with one another, and all of the interior textures are also positively correlated

Table 3. Percentage variance (eigenvalues) and character of first four components.

Component	Component variance as proportion of total dataset variance (%)	Interpreted texture type
PC1	55.24	Edge
PC2	21.56	Interior
PC3	12.79	Edge
PC4	7.58	Interior
PC5-8	Total of components 5-8 = 3.13	Not used

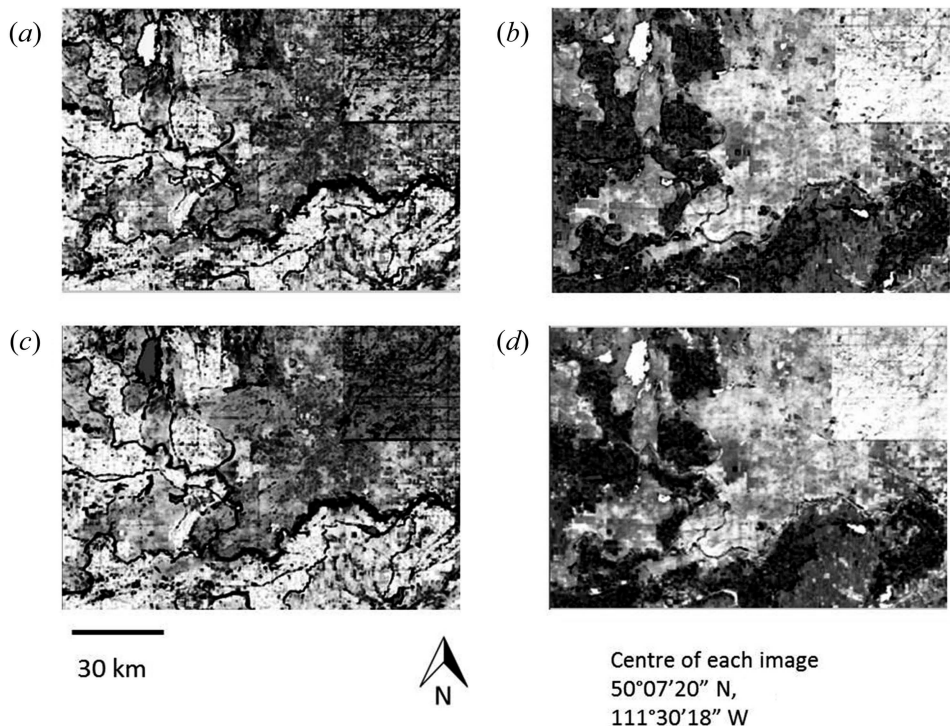


Figure 2. Principal component images 1–4 of AB image, 25×25 neighbourhood. (a) PC1, (b) PC2, (c) PC3, (d) PC4. PC1 and PC3 highlight edges, PC2 and PC4 highlight interiors. Note that 'highlight' may appear either bright or dark on the images. North and scale bar apply to all sections.

with one another. In PC1, those textures that are highly correlated with any others have higher loadings, while Cor and Mean, not highly correlated with other textures, have loadings near 0. Since all image pixels are used to calculate both PCA and the correlation matrix, both PC1 and the matrix are most heavily influenced by the textures of groups of pixels (classes), occupying the largest area on the image. A generalization that comes from this empirical observation, although it is consonant with what would be predicted from knowledge of the edge and interior textures alone, leads to the second hypothesis

Hypothesis 2: PC1 (from Hypothesis 1, PC1 will be an edge component) oppositely loads edge and interior textures.

It is not predictable whether the edge textures will be positively or negatively weighted, only that they will all have the same sign. If edge textures are positively loaded, edges will appear bright on the component, and if negatively correlated, they will appear dark.

The other edge component is PC3: this would represent a different pattern of edges, one that is less prominent on this image. It is heavily negatively loaded by ASM, Var, and Con and moderately positively loaded by Cor, Ent, and Mean. ASM contrasted with Ent is expected in an edge component. Con contrasted with Cor and Mean is also expected in an edge component. Both of these are predicted from Hypothesis 2. Cor and mean,

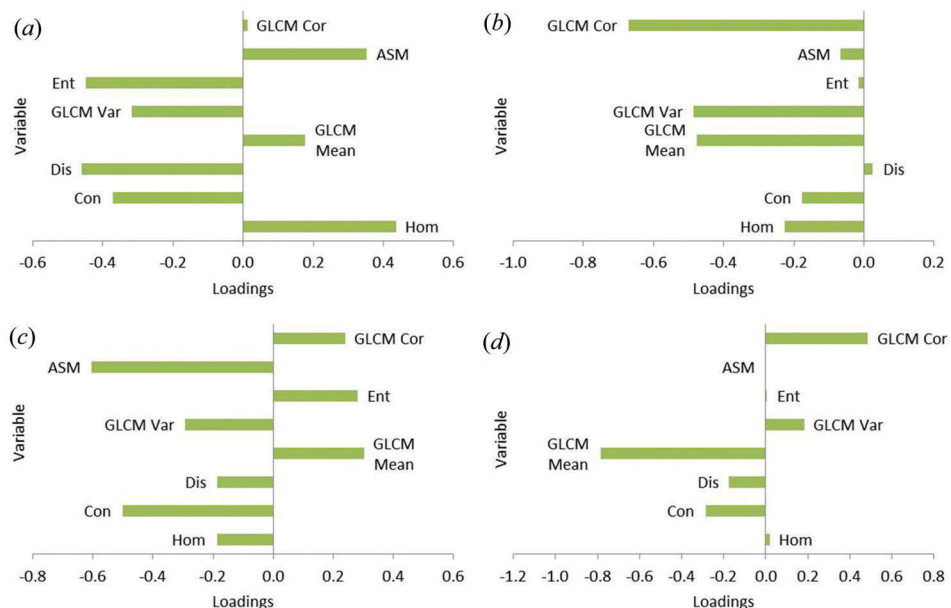


Figure 3. Loadings (correlations between individual input bands and output component) for PC 1–4, AB image, 25×25 neighbourhood. (a) PC1, edge texture, 55.3% of dataset variance; (b) PC2, interior texture, 21.6% of dataset variance; (c) PC3, edge texture, 12.8% of dataset variance; (d) PC4, interior texture, 7.6% of dataset variance. For an explanation of loadings, please see Section 1.4 of this article.

Table 4. Correlation matrix of input texture measures, AB image, 25×25 neighbourhood size.

	Cor	ASM	Ent	Var	Mean	Dis	Con	Hom
Cor	1.00	-0.04	0.07	0.50	0.40	-0.14	-0.02	0.23
ASM		1.00	-0.84	-0.27	0.16	-0.59	-0.28	0.78
Ent			1.00	0.56	-0.25	0.86	0.86	-0.93
Var				1.00	-0.03	0.65	0.65	-0.36
Mean					1.00	-0.35	-0.35	0.45
Dis						1.00	-0.87	-0.88
Con							1.00	-0.53
Hom								1.00

Correlations expected from texture equations are in boldface. Labels in boldface are 'edge' textures.

interior components, contrasted with ASM, also an interior component, are less expected but might indicate an edge where two different patches, each with a different interior texture, adjoin one another within the window. ASM (highly negatively correlated with Ent) might be expected to vary from image to image, depending on the interior textures of the classes present, and be less amenable to generalization.

PC2 is an interior component. All highly loaded texture measures have the same sign, in this case negative. If all were positive, the image would be its photographic negative: the important thing is the same sign for all prominently loaded textures. Three textures dominate the loadings: Cor, Var, and Mean. Cor and Mean are interior textures, and their heavy loading into an interior component is expected. Var was identified from its equation to be possibly an edge texture, but its important inclusion in an interior

component means that Var will need to be examined in other images. PC4, the other interior component, is also heavily loaded by Cor and Mean, although in this case, they have opposite signs (in other words are contrasted with one another). As seen in the analysis of PC3, it is quite plausible that different interior textures have different relationships between Cor and Mean, and that these be separated into different components. A plausible generalization, from the loadings of PC2, PC3, and PC4, is

Hypothesis 3: Cor and Mean figure prominently in interior components.

Their signs and relative importance will depend on the particular patch interior textures for the land covers in the image and are therefore not predictable. That they are important is predictable.

The analysis has also left questions to be clarified using other images with different patch textures

Hypothesis 4: Ent is unpredictable and may be an 'independent' texture whose utility depends on the particular texture of the land-cover patches.

'Independent' here means that Ent contains spatial information of a nature that is not ordinarily highly correlated with and single texture or combination of other textures in most images. This can be seen to some extent by examining the correlation measures in [Tables 4, 5, and 7](#): no consistent pattern of correlations for Ent emerges across the several images.

Hypothesis 5: Var is unpredictable according to our edge/interior texture classification, but it appears to figure prominently in components with high Cor and Mean.

2.2 Hypothesis testing 1: other images

These five hypotheses will now be compared for 25×25 pixel neighbourhoods for the GR and LB images.

2.2.1. GR image 25×25 pixel neighbourhood

The GR image ([Figure 1](#)) contains very different objects from the AB image. The sea portion has dense lines and edges throughout, some of which may be image noise. It is difficult to visually distinguish the 'interior' of sea objects at this resolution. The land area is easier to divide into edge and interior, with edges representing shadows and interiors

Table 5. Correlations among bands, GR25 image, 25×25 neighbourhood size.

	Cor	ASM	Ent	Var	Mean	Dis	Con	Hom
Cor	1.00	0.07	0.09	0.47	0.10	-0.05	0.03	0.09
ASM		1.00	-0.98	-0.87	0.22	-0.95	-0.93	0.97
Ent			1.00	0.85	-0.16	0.94	0.92	-0.96
Var				1.00	-0.16	0.82	0.85	-0.77
Mean					1.00	-0.16	-0.18	0.23
Dis						1.00	0.99	-0.98
Con							1.00	-0.94
Hom								1.00

Correlations expected from texture equations are in boldface. Labels in boldface are 'edge' textures.

representing snow/ice covered mountains and bare rock. The shoreline is the most obvious edge feature. Because of these difficulties, the visual cue for assigning a component to 'edge' or 'interior' is the appearance of a prominent bright or dark line marking the shore. By this criterion, PC1 and PC2 are edge components and PC3 is an interior component. [Table 5](#) shows texture correlations for GR25. As is the case for AB25, the most highly correlated textures in [Table 5](#) are also heavily loaded to PC1. The correlations of Ent with other textures differ from those in AB25, pointing out that Ent behaves differently in different images. [Table 6](#) shows variance and component assignment. Edge components account for 70.44% of total variance, and interior 27.12%; this supports Hypothesis 1. The percentage of dataset variance decreases rapidly, falling to only 1.45% for PC4, indicating that this image is structurally simpler, meaning that fewer variance patterns dominate most of the image area.

[Figure 4](#) shows the first three components; [Figure 5](#) shows the loadings for these components. PC1 heavily negatively loads the four edge textures Ent, Var, Dis, and Con. ASM and Hom, interior textures, are heavily positively loaded, while the other two interior textures, Cor and Mean, figure hardly at all. These observations support Hypothesis 2.

For GR25, PC2 and PC3 are the interior components. PC2 strongly loads Cor, Var, and Mean, all with the same sign. This is the same trio that loaded PC2 in AB25. PC3 very heavily loads Mean and shows a minor contrast of Mean with Cor. Both PC2 and PC3 support Hypothesis 3.

Ent does not figure prominently outside of PC1; in PC1, it aligns with the edge textures. It does figure prominently (contrasting with ASM) in PC4 and PC6; however, these components represent a negligible portion of dataset variance. Ent does not appear to be an important texture for this image. This corroborates the unique and unpredictable status of Ent, thus supporting Hypothesis 4. Var behaves in the same way as for AB25, leaving ambiguous that whether Var is an edge or interior texture. Although Var follows Mean and Cor, it does not have an independent role in this image. This supports Hypothesis 5.

Table 6. Percentage variance and character of first 4 components, GR25 image.

Component	Component variance as proportion of total dataset variance (%)	Interpreted texture type
PC1	70.44	Edge
PC2	15.81	Interior
PC3	11.31	Interior
PC4-8	Total of components 4-8 = 2.44	Not used

Table 7. Correlations among bands, GR25 image, 25 × 25 neighbourhood size.

	Cor	ASM	Ent	Var	Mean	Dis	Con	Hom
Cor	1.00	-0.02	-0.07	0.03	-0.34	-0.32	-0.29	0.31
ASM		1.00	-0.84	-0.52	-0.15	-0.56	-0.40	0.75
Ent			1.00	0.80	0.17	0.85	0.70	-0.95
Var				1.00	0.29	0.89	0.89	-0.76
Mean					1.00	0.32	0.36	-0.23
Dis						1.00	0.96	-0.91
Con							1.00	-0.76
Hom								1.00

Correlations expected from texture equations are in boldface. Labels in boldface are 'edge' textures.

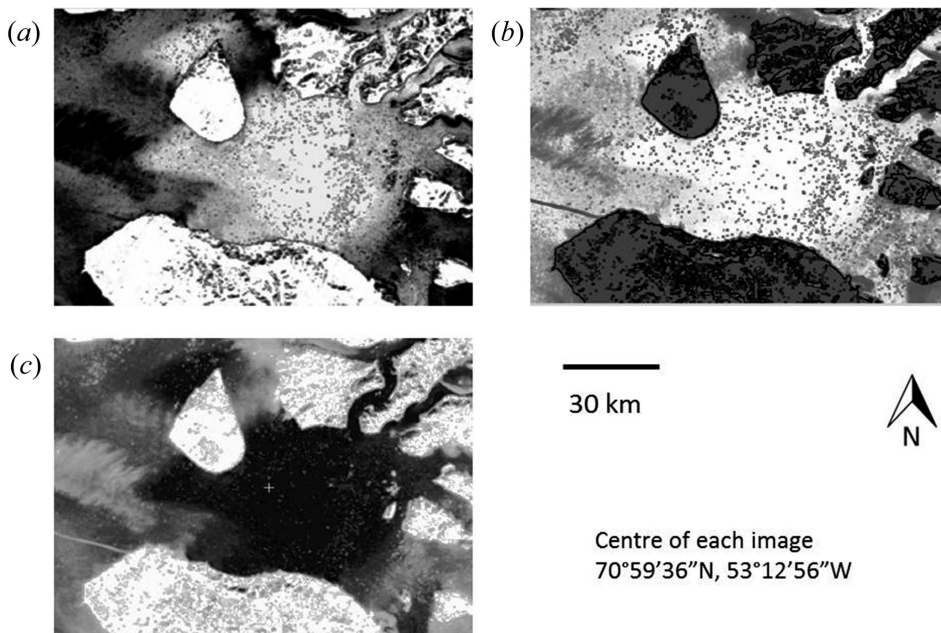


Figure 4. Principal component images 1–3 of GR image, 25×25 neighbourhood. (a) PC1, (b) PC2, (c) PC3. PC1 is an edge component; PC2 and PC3 are considered interior components, although PC2 is ambiguous. North and scale bar apply to all sections.

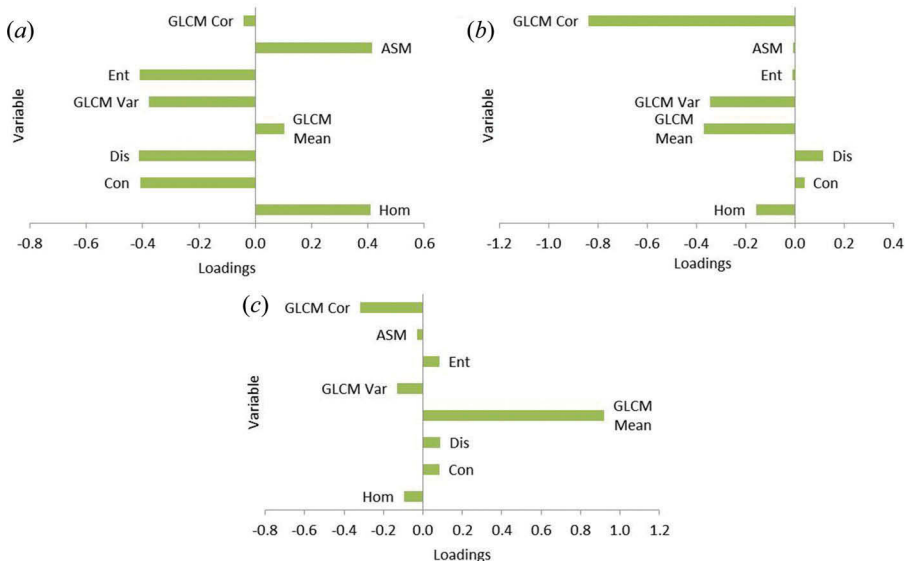


Figure 5. Loadings for PC1–3, GR image, 25×25 neighbourhood. (a) PC1, edge texture, 70.4% of dataset variance. (b) PC2, interior texture, 15.8% of dataset variance. (c) PC3, interior texture, 11.3% of dataset variance. For an explanation of loadings, please see Section 1.4 of this article.

2.2.1.1. Summary of the AB25–GR25 comparison. Comparing AB25 with GR25, we find that PC1 behaves similarly in both. PC2 in both is heavily loaded with Cor and Mean, both having the same sign. PC3 is heavily loaded with Cor and Mean having opposite signs. All hypotheses are supported.

2.2.2. Libya image, 25 × 25 neighbourhood

The northern half of the LB image is occupied by sand dunes, with many irregular visual edges. The southern half, showing bare rock, has many longer and curved edges, but also some larger more uniform areas. The density of edges in the northern part of the image makes it difficult to discern whether a given component is more edge or more interior, since in the north, the edges seem to be ubiquitous and not to mark class patch borders. The visual criterion used to distinguish edge and interior components is the presence of obvious lines in the southern half of the image. Because of the textural complexity of the northern area, it is very difficult to separate edge from interior, and it is expected that smaller neighbourhood sizes might have quite different behaviour than the 25 × 25 neighbourhood size. This is a case where the definition of a land-cover class may be strongly determined by spatial resolution. [Table 7](#) shows the texture correlation matrix for the LB25 image; [Table 8](#) shows variance distribution and component assignment. Observations from the correlation matrix support those for the GR25 image: Ent behaves unlike it does in the others, as expected; the other observations are similar to the AB25 image. Edge components account for 62.89% of dataset variance and interior for 35.05%. This supports Hypothesis 1 – however, see [Section 2](#) about what constitutes a patch that can be said to have an ‘interior’.

[Figure 6](#) shows the component images and [Figure 7](#) shows the loadings. PC1 loadings reveal the interior textures ASM and Hom to be negatively loaded, contrasting with the edge textures Ent, Var, Dis, and Con. Cor and Mean are less important in this pattern, although Mean is more heavily loaded than in the AB or GR images. These observations together support Hypothesis 2.

As with the AB and GR images, LB PC2 loads heavily with Cor and Mean, although with opposite signs from AB and GR. ASM loads negatively as does Mean. Ent and Cor both load positively. Thus, ASM and Ent maintain their expected opposite signs. PC3 for this image seems more like PC2 for the AB and GR images, with Cor and Mean loaded with the same sign. However, in the LB image, PC3 has very high loadings for almost all textures, with only Ent loading to the opposite sign. In other words, PC3 singles out Ent as being uniquely important. This supports Hypothesis 4 and indicates Ent to be particularly important in this image, while GR’s PC3 also supported Hypothesis 4 and had Ent as unimportant. Thus, Ent’s sensitivity to the actual patch textures of individual images is upheld.

Table 8. Percentage variance and character of top 4 components, LB25 image.

Component	Component variance as proportion of total dataset variance (%)	Interpreted texture type
PC1	62.89	Edge
PC2	16.85	Interior
PC3	9.53	Interior
PC4	8.67	Interior
PC5-8	Total of components 5–8 = 2.06	Not used

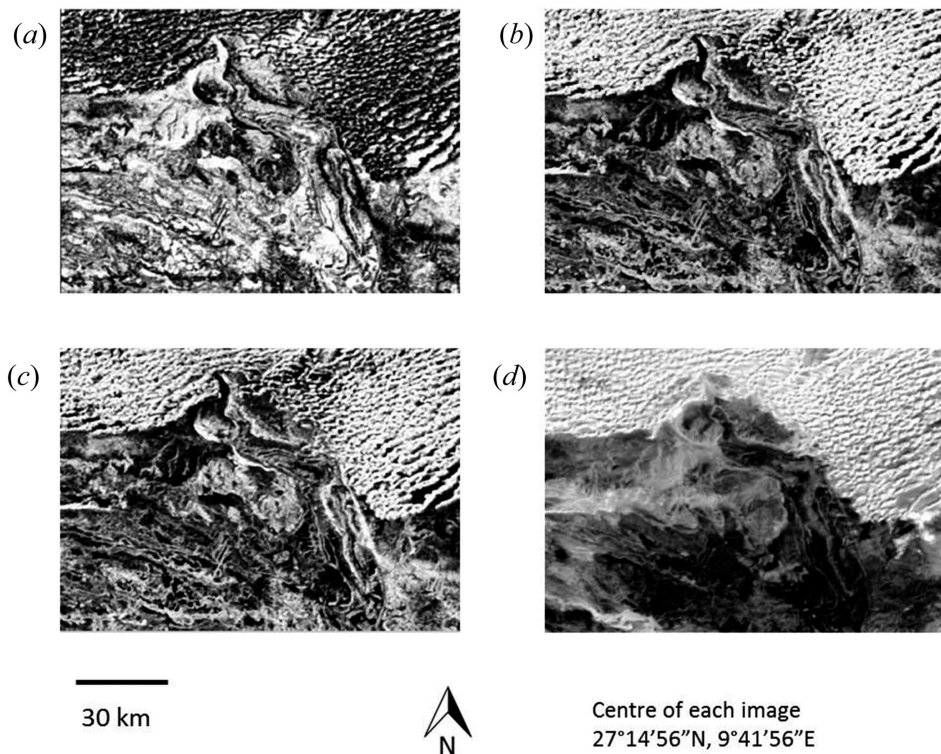


Figure 6. Principal component images 1–3 of LB image, 25×25 neighbourhood. (a) PC1, (b) PC2, (c) PC3, (d) PC4. PC1, PC2, and PC3 are edge components and PC4 is an interior component. North and scale bar apply to all sections.

PC4 is characterized by a strong contrast between Mean and ASM. Dark areas on the image, corresponding to neighbourhoods containing pixels with high MEAN and simultaneously low ASM, occur in the southern part of the image. Cor is not heavily loaded. The Mean loading supports Hypothesis 3, but Cor does not.

Var remains ambiguous in the first four components. It figures prominently and independently in component 6, with only 0.6% of dataset variance. This supports Hypothesis 5 but agrees with the GR image that Var might be important for classes occupying very small areas.

2.2.2.1. Summary of the comparison of LB25 to AB25 and GR25. The LB image is somewhat different in texture from both AB and GR images. There is ambiguity about what can be called an ‘interior.’ Nevertheless, similar loading patterns appear to those in AB25 and GR25, supporting the hypotheses.

2.3. Hypothesis testing II: other neighbourhood sizes

The detailed reasoning for the support or lack of it for the 25×25 neighbourhood has been presented above; the same procedure applies to the other neighbourhood sizes, and in the interest of space, only a summary will be presented for the smaller windows

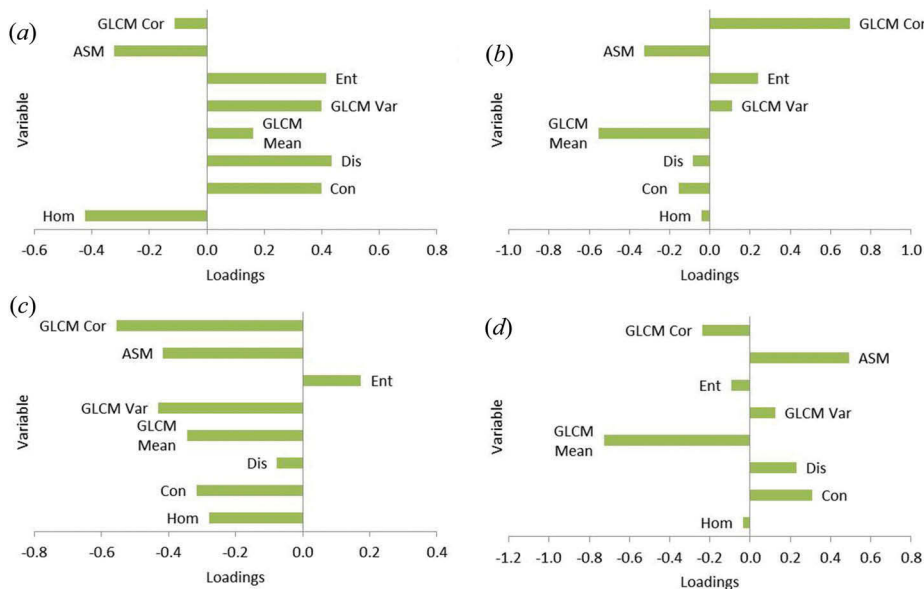


Figure 7. Loadings for PC 1–4, LB image, 25 × 25 neighbourhood. (a) PC1, edge texture, 62.9% dataset variance; (b) PC2, interior texture, 16.9% dataset variance; (c) PC3, interior texture, 9.5% dataset variance; (d) PC4, interior texture, 8.7% dataset variance. For an explanation of loadings, please see Section 1.4 of this article.

except where something different from the 25-sized neighbourhoods is observed. Figures and tables are similarly abbreviated, and the correlation matrices are not reproduced as they do not add anything new to the discussion.

2.3.1. Alberta image

2.3.1.1. 13 × 13 Neighbourhood (AB13). Table 9 shows importance of the edge and interior components, confirming Hypothesis 1. Loadings for the 25, 13, and 5 neighbourhood images in PC1 (edge component) can be found in Figure 8 and for PC2 (interior component) in Figure 9.

AB13 shows no substantial difference from AB25. The same numbered components are judged to be edge and interior. The edge components account for much higher percentage of dataset variance than do interior components, supporting Hypothesis 1. The pattern of loadings is essentially the same as in AB25, with minor differences in

Table 9. Percentage variance and character of first 4 components, AB image 13 × 13 and 5 × 5.

Component	Component variance as proportion of total dataset variance (%)		Interpreted texture type	Component variance as proportion of total dataset variance (%)		Interpreted texture type
	AB13	AB13		AB5	AB5	
PC1	58.46		Edge	59.80		Edge
PC2	17.91		Interior	15.00		Interior
PC3	12.76		Edge	13.21		Edge
PC4	8.24		Interior	9.40		Interior
PC5–8	Total of components 5–8 = 2.63		Not used	Total of components 5–8 = 2.60		Not used

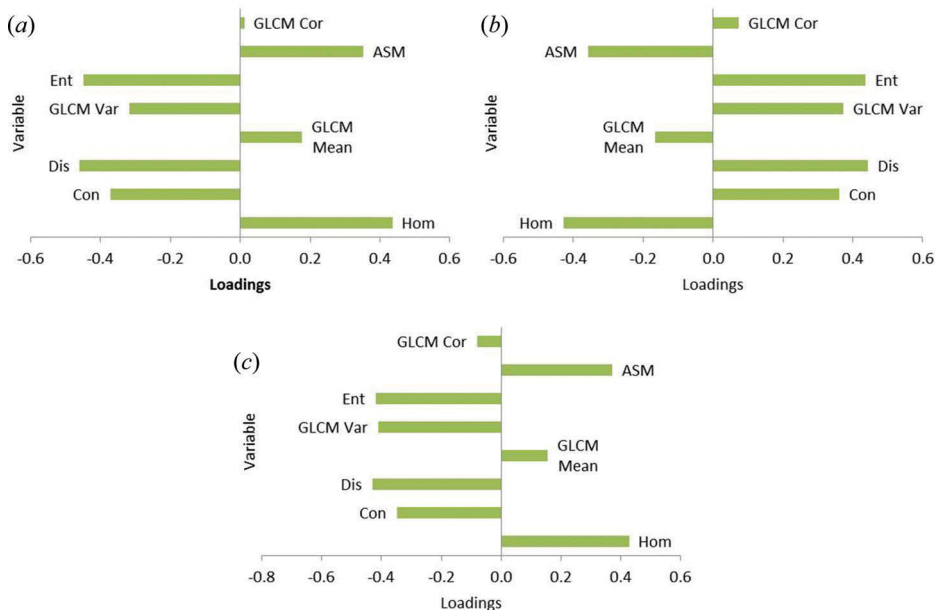


Figure 8. Comparison of loadings of PC1, AB image, (a) 25×25 neighbourhood, (b) 13×13 neighbourhood, and (c) 5×5 neighbourhood. For an explanation of loadings, please see Section 1.4 of this article.

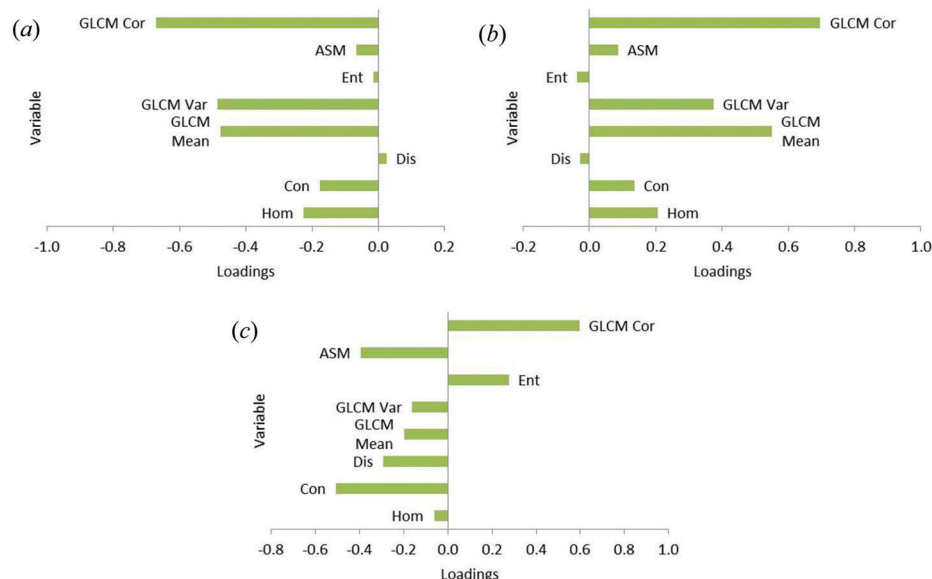


Figure 9. Comparison of loadings of PC2, AB image, (a) 25×25 neighbourhood, (b) 13×13 neighbourhood, and (c) 5×5 neighbourhood. For an explanation of loadings, please see Section 1.4 of this article.

numeric values. The signs of the loadings are flipped in some components as compared to those AB25, but the same textures are contrasted with one another (opposite signs). This results in a particular ground cover being bright in one image where it is dark in the other, but it is distinct and recognizable in both. AB13 conforms to observations for AB25; so all hypotheses are upheld.

2.3.1.2. 5×5 Neighbourhood (AB5). Table 8 confirms Hypothesis 1. Loadings for PC1 and PC2 for all neighbourhood sizes are in Figures 8 and 9, respectively. While PC1 is essentially the same for the three neighbourhood sizes, in PC2 and PC4, the loadings for AB5 differ substantially from those for AB25 and AB13 (Figure 8). Despite this, in PC2 and PC4, Ent along with either Cor or Mean all load with opposite sign from all the other textures. This supports Hypothesis 3 that Cor and Mean figure strongly in interior components; it also adds unpredictable behaviour for Ent, confirming Hypothesis 4.

2.3.1.3. Summary of the comparison of AB25 with AB13 and AB5. AB13 and AB5 both support the hypotheses formulated based on the AB25 image. The differing neighbourhood sizes do not change the textures for this set of land covers and patches.

2.3.2. GR image

GR13 and GR5 loadings for both edge and interior components show no essential difference between them nor with GR25. The only notable feature is that, as in AB, the loadings signs are reversed for GR25 as compared to the other two GR sizes. The information content remains the same: the images are approximate photographic negatives of one another. Edge components continue to dominate the dataset variance. Therefore, conclusions about the hypotheses stated in the section 2.2.1 also hold for the other GR neighbourhood sizes.

2.3.3. LB image

For both LB13 and LB5, the AB and GR patterns are continued, i.e. the same information and a reversal of loadings signs. The complex visual texture in the northern half of LB led above to a question about greater differences among neighbourhood sizes for this image. This difference shows in PC3 (Figure 10). As the neighbourhood size becomes smaller, the % dataset variance in this component rises. In PC3 for LB25, Ent stands alone. For LB13 and LB5, Ent allies with Mean, and Mean becomes more important. The loading signs reverse between LB13 and LBV5, but here again contrasting loadings are maintained between PC2 and PC3.

In summary, the LB images uphold the hypotheses and confirm that Ent is important in this 'edgy' land cover.

2.4. Summary of hypotheses and generalizations

Five hypotheses were derived from observation of the AB 25×25 image. Table 10 shows the support and contra-indications from the other AB neighbourhood sizes and from the GR and LB images at all three neighbourhood sizes. The support is remarkably uniform, indicating that it is indeed possible to extract generally applicable texture guidelines for very different land covers and neighbourhood sizes.

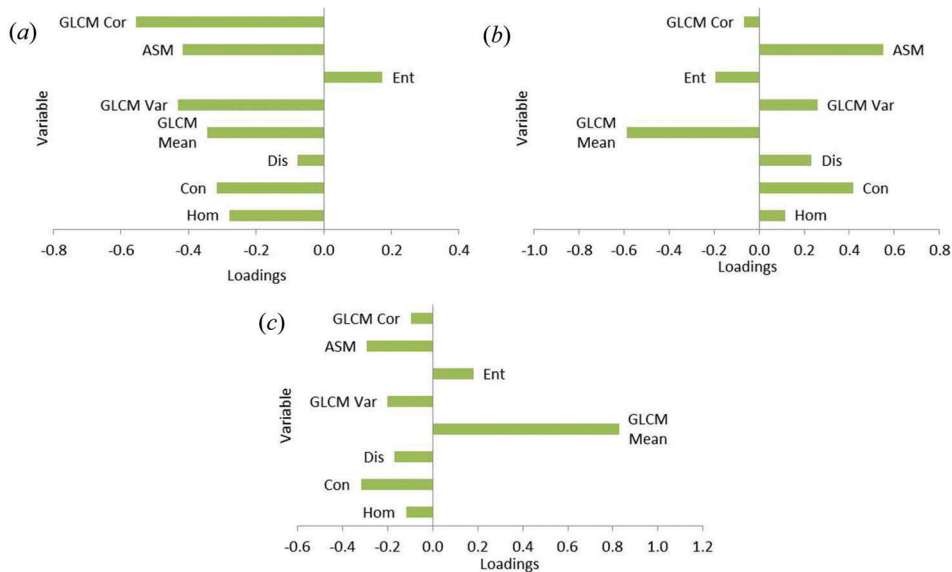


Figure 10. Comparison of loadings of PC3, LB image, (a) 25×25 neighbourhood, (b) 13×13 neighbourhood, and (c) 5×5 neighbourhood. This image shows distinct patterns for smaller neighbourhoods. For an explanation of loadings, please see Section 1.4 of this article.

Table 10. Matrix of support for hypotheses by test image..

Image and scaleHypothesis	GR25	LB25	AB13	GR13	LB13	AB5	GR5	LB5
1	Y	Y	Y	Y	Y	Y	Y	Y
2	Y	Y	Y	Y	Y	Y	Y	Y
3	Y	Y	Y	Y	Y	Y	Y	Y
4	Y	Y	Y	Y	Y	Y	Y	Y
5	Y ¹	Y ¹	Y	Y	Y	Y	Y	Y

1, Var appears independent only in late components representing very small percentage of dataset variances. Y, Supports hypothesis; N, does not support hypothesis.Hypothesis 1: Edge components account for a much larger percentage of total dataset variance than interior components; PC1 will be an edge component.Hypothesis 2: PC1 will oppositely load edge and interior textures.Hypothesis 3: Cor and Mean will figure prominently in interior components.Hypothesis 4: Ent is unpredictable and may relate to particular land covers.Hypothesis 5: Var is unpredictable but does not behave independently of other measures

Figure 11 summarizes graphically the importance of each texture measure in the interior and edge components.

2.4.1. Choosing an interior texture

It is clear that Cor and Mean are important for interiors. They can occur with different importance and relationships to one another in different interior components, showing that they are likely to have different values in different parts of the image. Of the two, Mean is slightly more consistently associated with interiors (Figure 11). When using a texture layer to improve classification accuracy, it is important to distinguish between different patch interior textures of the desired classes. A proposed first guideline is

Guideline 1: When using texture for classification, use GLCM Mean as a first choice and GLCM Cor as a possible addition.

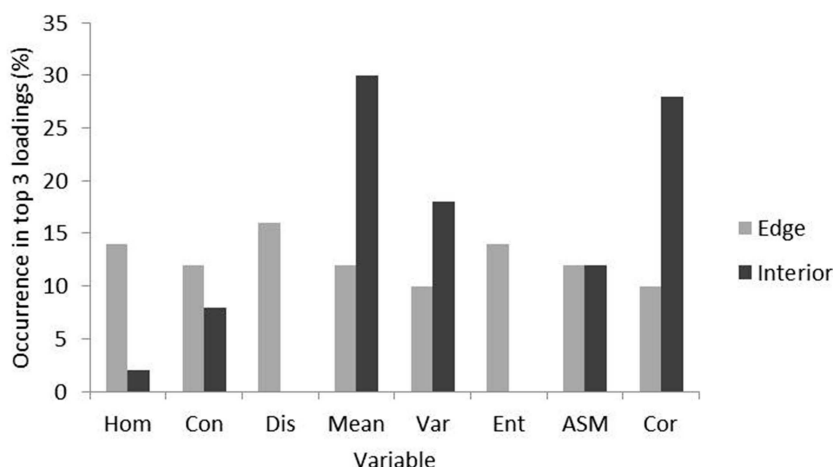


Figure 11. Relative frequency of occurrence of each texture measure in the highest three loadings for interior and edge components, for all images and neighbourhood sizes. Only are PC1–4 considered (PC1–3 for GR image).

It needs to be emphasized that Mean refers to Haralick's *GLCM Mean*, not to the mean of pixel values within the neighbourhood. GLCM Mean is the mean of probability of co-occurrence of specific DN values within the neighbourhood. This is important in selecting algorithms, because a 'mean' convolution algorithm usually also exists in software, whose primary purpose is either to remove image noise or to degrade spatial resolution. This can be confusing whether care is not taken to look for GLCM Mean. A similar confusion can exist between GLCM Cor and an algorithm with a different purpose-labelled 'correlation.'

The Mean and Cor formulae (Table 2) do not include a weight differentiating large from small DN differences in adjacent pixels. Therefore, neither Mean nor Cor acts as an edge component. Why does Cor not occur as consistently as Mean in interior images? It is conceptually plausible that some interior textures have a high and some have a low predictability. Thus, Cor might figure prominently in the interior components of some images and not in others. This leaves Mean as a more consistent indicator of interior textures over many landscapes.

2.4.2. Choosing an edge texture

No single texture stands out as diagnosing edge components. This is because image edges are dominated by PC1, and all PC1s show a fairly even balance between all edge textures contrasting with all interior textures. It would seem that any pair of one edge and one interior texture should work equally well at defining edges. Probably, Ent should not be included among the edge textures, due to its odd behaviour (Hypothesis 4). If Mean is already chosen as an interior texture, and Ent (and Var) behaves unpredictably, then it would make sense to choose one of Con or Dis to enhance edges on the image. Of the two, Con creates a larger range of values. This

could also be accomplished by judicious rescaling of Dis; however, so there is not much to choose between the two. To avoid rescaling, choose Con.

The question remains whether an edge texture will aid in classification. This depends on the nature and spatial scale of the ground cover patches. Some, like dunes in LB, might have many visual edges within the boundaries of what the analyst defines as a cover patch. In this case, creating a class signature containing an edge texture would be useful. If the edges only serve to outline patches, then an edge texture cannot be expected to increase class accuracy. As noted above, edge textures might be very useful as base data on which to perform an object segmentation algorithm: this proposal deserves further empirical investigation. The proposed guideline for edges is

Guideline 2: If a class is characterised by edges within its patch boundaries, choose Con. If no class has this characteristic, then an edge texture unlikely to be helpful for classification. Con might be used in automated object creation.

2.4.3. Using Ent

Ent, while usually an edge texture and always contrasted with ASM where either one is highly loaded, cannot be invariably associated with either edge or interior components. Ent is a measure of the randomness of pixel associations. Ent appears to be a single texture which might be able to characterize a particular ground cover within an image. Ent might also take on different values for edges with different characteristics. Ent occurs in PCA images either not at all in the first components or in a particular component later in the series. Its position of importance likely indicates that it is diagnostic of a particular class, different in each image, whose importance varies with the areal extent of that class.

Guideline 3: When doing detailed analysis of individual class textures, try Ent.

Guideline summary: For classification problems, choose Mean and, where a class patch is likely to contain edge-like features within it, Con. Cor is an alternative for Mean in these situations; Dis may similarly be used in place of Con. For more detailed texture study, add Ent.

2.5. Discussion

These results confirm what has been found in studies that engage in extensive texture comparisons with the aim of selecting the specific measures that will most improve classification accuracy. Notably, Murray et al. found the use of Mean, Con, and Ent, which provided the best accuracy for tundra vegetation using IKONOS imagery [29]. Their procedure selected the same measures as recommended here despite working with a different resolution and land cover. Ozdemir, Mert, and Senturk (2012) found Ent to be uniquely useful in relation to landscape patch metrics. Ozdemir and Karnieli (2011) found Con to be highly relevant in predicting forest structural parameters at high spatial resolution. This is a situation where the textures within patches are the subject of investigation, corroborating Guideline 2 of the current research.

Are the other commonly implemented Haralick textures of any use? This article attempts to arrive at broadly generalizable ways of choosing the textures most likely to be of use. The rules are intended for analysts wishing to add spatial to spectral

information for classification purposes. It is an improvement on 'choose something, anything.' Var and ASM do not appear in this analysis to perform any unique function. Hom dropped out of consideration since it serves mainly to contrast with Con and/or Dis in edge components. Con can serve this purpose alone to highlight edges.

This work has served to systematize and test the selection of textures. The rules have been proposed to encourage the non-expert to profit from the potential accuracy improvement by adding continuous spatial data to spectral information. This study has not demonstrated that adding these recommended textures to the various images actually improves accuracy, nor that they would necessarily improve accuracy more than other textures would do. It has demonstrated with the LB image that how one defines a class patch might influence the ability of texture to characterize it. It would be a very ambitious project to test these rules, with measured accuracies, on a wide variety of classes and textures in many landscapes. It is to be hoped that researchers who decide to include texture in their classifications will report accuracies with and without texture and specify the texture measure(s) chosen, rather than simply reporting the most successful trial. In that way over a long time period, such reports will appear in the literature and eventually allow a review leading to proven-reliable generalizations. If the current article encourages researchers to include texture, it will have helped hasten the day when that review can be written.

3. Conclusions

PCA of eight Haralick GLCM textures has been applied to three Landsat images of very different landscapes, using three neighbourhood sizes. Commonalities among the (data-dependent) results confirm the division of textures into those highlighting edges and those serving to distinguish different textures in patch interiors. This division agrees with predictions made on the basis of the texture equations. The generalizations, for all images and neighbourhood sizes, have allowed the creation of three practical guidelines for researchers wishing to include the spatial information provided by texture in image classifications but not able to engage in a detailed texture analysis. These guidelines are summarized as 'For classification problems, choose Mean and, where a class patch is likely to contain edge-like features, Con. Cor is an alternative for Mean in these situations; Dis may similarly be used in place of Con. For more detailed texture study, add Ent.'

Exhaustive empirical testing of these guidelines and their interaction with potential accuracy improvements is not possible within the confines of a single project but will rely on the accumulation of reported data from classifications in many landscapes and at many image resolutions. The identification of Con as the single most appropriate edge texture suggests its use as a substrate in automated object-creation algorithms.

Disclosure statement

No potential conflict of interest was reported by the author.



References

- Cao, X., J. Han, S. Yang, D. Tao, and L. Liao. 2016. "Band Selection and Evaluation with Spatial Information." *International Journal of Remote Sensing* 37: 4501–4520. doi:[10.1080/01431161.2016.1214301](https://doi.org/10.1080/01431161.2016.1214301).
- Chen, Q., and P. Gong. 2004. "Automatic Variogram Parameter Extraction for Textural Classification of the Panchromatic IKONOS Imagery." *IEEE Transactions on Geoscience and Remote Sensing* 42: 1106–1115. doi:[10.1109/TGRS.2004.825591](https://doi.org/10.1109/TGRS.2004.825591).
- Coburn, C. A., and A. C. B. Roberts. 2004. "A Multiscale Texture Analysis Procedure for Improved Forest Stand Classification." *International Journal of Remote Sensing* 25: 4287–4308. doi:[10.1080/0143116042000192367](https://doi.org/10.1080/0143116042000192367).
- Colombo, R., D. Bellingeri, D. Fasolini, and C. M. Marino. 2003. "Retrieval of Leaf Area Index in Different Vegetation Types Using High Resolution Satellite Data." *Remote Sensing Reviews* 86: 120–131. doi:[10.1016/S0034-4257\(03\)00094-4](https://doi.org/10.1016/S0034-4257(03)00094-4).
- Dong, P. 2000. "Test of a New Lacunarity Estimation Method for Image Texture Analysis." *International Journal of Remote Sensing* 21: 3369–3373. doi:[10.1080/014311600750019985](https://doi.org/10.1080/014311600750019985).
- Dorigo, W., A. Lucieer, T. Podobnikara, and A. Carnid. 2012. "Mapping Invasive *Fallopia Japonica* by Combined Spectral, Spatial, and Temporal Analysis of Digital Orthophotos." *International Journal of Applied Earth Observation and Geoinformation* 19: 185–195. doi:[10.1016/j.jag.2012.05.004](https://doi.org/10.1016/j.jag.2012.05.004).
- Eastman, J. R., and M. Fulk. 1993. "Long Sequence Time Series Evaluation Using Standardized Principal Components." *Photogrammetric Engineering and Remote Sensing* 69: 991–996.
- Eklundh, L., and A. Singh. 1993. "A Comparative Analysis of Standardised and Unstandardized Principal Component Analysis in Remote Sensing." *International Journal of Remote Sensing* 14: 1359–1370. doi:[10.1080/01431169308953962](https://doi.org/10.1080/01431169308953962).
- Emerson, C., N. Lam, and D. Quattrochi. 2005. "A Comparison of Local Variance, Fractal Dimension, and Moran's I as Aids to Multispectral Image Classification." *International Journal of Remote Sensing* 26: 1575–1588. doi:[10.1080/01431160512331326765](https://doi.org/10.1080/01431160512331326765).
- Ferro, C. J. S., and T. A. Warner. 2002. "Scale and Texture in Digital Image Classification." *Photogrammetric Engineering and Remote Sensing* 68: 51–63.
- Franklin, S. E., R. J. Hall, L. M. Moskal, and M. B. Lavigne. 2000. "Incorporating Texture into Classification of Forest Species Composition from Airborne Multispectral Images." *International Journal of Remote Sensing* 21: 61–79. doi:[10.1080/014311600210993](https://doi.org/10.1080/014311600210993).
- Gonzalez, R. C., and R. E. Woods. 1992. *Digital Image Processing*. Boston: Addison-Wesley.
- Hall-Beyer, M. 2003. "Comparison of Single-Year and Multi-Year NDVI Time Series Principal Components in Cold Temperate Biomes." *IEEE Transactions on Geoscience and Remote Sensing* 41: 2568–2574. doi:[10.1109/TGRS.2003.817274](https://doi.org/10.1109/TGRS.2003.817274).
- Hall-Beyer, M. 2007. *GLCM Texture Tutorial*. <http://www.fp.ucalgary.ca/mhallbey/tutorial.htm>, 2007. Accessed on 16 May 2016.
- Haralick, R. M. 1979. "Statistical and Structural Approaches to Texture." *Proceedings of the IEEE* 67:786–804.
- Haralick, R. M., K. Shanmugam, and I. Dinstein. 1973. "Textural Features for Image Classification." *IEEE Transactions on Systems, Man and Cybernetics* 3: 610–621. doi:[10.1109/TSMC.1973.4309314](https://doi.org/10.1109/TSMC.1973.4309314).
- Jensen, J. R. 2007. *Remote Sensing of the Environment: An Earth Resource Perspective*. Upper Saddle River: Pearson Prentice Hall.
- Jolliffe, I. T. 2002. *Principal Component Analysis*. 2nd ed. New York: Springer.
- Kim, M., M. Madden, and T. A. Warner. 2009. "Forest Type Mapping Using Object-Specific Texture Measures from Multispectral Ikonos Imagery: Segmentation Quality and Image Classification Issues." *Photogrammetric Engineering and Remote Sensing* 75: 819–829. doi:[10.14358/PERS.75.7.819](https://doi.org/10.14358/PERS.75.7.819).
- Laurin, G. V., V. Liesenberg, Q. Chen, L. Guerrieri, F. DelFrate, A. Bartolini, D. Coomes, B. Wilebore, J. Lindsell, and R. Valentini. 2013. "Optical and SAR Sensor Synergies for Forest and Land Cover Mapping in a Tropical Site in West Africa." *International Journal of Applied Earth Observation and Geoinformation* 21: 7–16. doi:[10.1016/j.jag.2012.08.002](https://doi.org/10.1016/j.jag.2012.08.002).

- Lillesand, T. M., R. W. Kiefer, and J. W. Chapman. 2007. *Remote Sensing and Image Interpretation*. 6th ed. Hoboken: John Wiley and Sons.
- Marceau, D. J., P. J. Howarth, J.-M. Dubois, and D. J. Graton. 1990. "Evaluation of the Grey-Level Co-Occurrence Matrix Method for Land-Cover Classification Using SPOT Imagery." *IEEE Transactions on Geoscience and Remote Sensing* 28: 513–519. doi:10.1109/TGRS.1990.572937.
- MathWorks graycoprops. 2012. *Properties of Gray-Level Co-Occurrence Matrix*. Mathworks Product Documentation Version R2012a, 2012, <http://www.mathworks.com/help/toolbox/images/ref/graycoprops.html>
- Murray, H., A. Lucieer, and R. Williams. 2010. "Texture-Based Classification of Sub-Antarctic Vegetation Communities on Heard Island." *International Journal of Applied Earth Observation and Geoinformation* 12: 138–149.
- Myint, R. W. 2003. "Fractal Approaches in Texture Analysis and Classification of Remotely Sensed Data: Comparisons with Spatial Autocorrelation Techniques and Simple Descriptive Statistics." *International Journal of Remote Sensing* 24: 1925–1947. doi:10.1080/01431160210155992.
- Myint, S. W., -N. S.-N. Lam, and J. M. Tyler. 2004. "Wavelets for Urban Spatial Feature Discrimination: Comparisons with Fractal, Spatial Autocorrelation, and Spatial Co-Occurrence Approaches." *Photogrammetric Engineering and Remote Sensing* 70: 803–812. doi:10.14358/PERS.70.7.803.
- Okubo, S., M. D. Parikesit, K. Harashina, K. Takeuchi, and M. Umezaki. 2010. "Land Use/Cover Classification of a Complex Agricultural Landscape Using Single-Dated Very High Spatial Resolution Satellite-Sensed Imagery." *Canadian Journal of Remote Sensing* 36: 722–736. doi:10.5589/m11-010.
- Ozdemir, I., and D. N. M. Donaghue. 2013. "Modelling Tree Size Diversity from Airborne Laser Scanning Using Canopy Height Models with Image Texture Measures." *Forest Ecology and Management* 295: 28–37. doi:10.1016/j.foreco.2012.12.044.
- Ozdemir, I., and A. Karnieli. 2011. "Predicting Forest Structural Parameters Using the Image Texture Derived from Worldview-2 Multispectral Imagery in a Dryland Forest, Israel." *International Journal of Remote Sensing* 13: 701–710.
- Ozdemir, I., A. Mert, and O. Senturk. 2012. "Predicting Landscape Structural Metrics Using ASTER Satellite Data." *Journal of Environmental Engineering and Landscape Management* 20: 168–176. doi:10.3846/16486897.2012.688371.
- PCI. 2013. *Geomatica Focus User's Manual*. http://www.ucalgary.ca/appinst/doc/geomatica_v91/manuals/focus.pdf.
- Pearlstine, L., K. M. Portier, and S. E. Smith. 2005. "Textural Discrimination of an Invasive Plant, *Schinus Terebinthifolius*, from Low Altitude Aerial Digital Imagery." *Photogrammetric Engineering and Remote Sensing* 71: 289–298. doi:10.14358/PERS.71.3.289.
- Rabia, A. H., and F. Terribile. 2013. "Semi-Automated Classification of Gray Scale Aerial Photographs Using Geographic Object Based Image Analysis (GEOBIA) Technique." *Geophysical Research Abstracts* 15: 219.
- Ricotta, C., and G. C. Avena. 2000. "The Remote Sensing Approach in Broad-Scale Phenological Studies." *Applied Vegetation Science* 3: 117–122. doi:10.2307/1478925.
- RSI. 2004. Research Systems Incorporated, 4990 Pearl East Circle, Boulder CO 80301. <https://www.harrisgeospatial.com/docs/ExtractFeatures.html>
- Rushing, J. A., H. S. Ranganath, H. K. Hinke, and S. J. Graves. 2001. "Using Association Rules as Texture Features." *IEEE Transactions on Pattern Analysis and Machine Intelligence* 23: 845–858. doi:10.1109/34.946988.
- Srinivasan, G., and G. Shobha. 2008. "Statistical Texture Analysis." *Proceedings of the World Academy of Science, Engineering and Technology* 36:1264–1269.
- Wang, L., C. Shi, C. Diao, J. Wenjie, and D. Yin. 2016. "A Survey of Methods Incorporating Spatial Information in Image Classification and Spectral Unmixing." *International Journal of Remote Sensing* 37: 3870–3910. doi:10.1080/01431161.2016.1204032.